DOI: 10.21062/mft.2022.080 http://www.journalmt.com

Processing of Deep-sea Nodules by Silicothermic Reduction

Klára Borkovcová (0000-0002-3133-6186), Pavel Novák (0000-0001-9947-2566), Eliška Chmelíková
University of Chemistry and Technology, Prague, Department of Metals and Corrosion Engineering, Technická 5, 166 28 Prague 6, Czech Republic. E-mail: borkovck@vscht.cz

Deep-sea nodules are ores formed on the sea floor at depths of 3000 to 6000 m as a result of sedimentation. They range in size from 1 cm to 15 cm and contain mainly manganese and iron and other elements that are collected from the nodules by complex pyrometallurgical and hydrometallurgical processes. These other elements of interest are bound in the nodules mainly in the form of manganese and iron oxides. In order to achieve a high yield of metals bound in nodules in the form of oxides, it is necessary to disintegrate this arrangement in the lattice. This can be achieved by exposing the deep-sea nodules to a reducing condition. This paper deals with the one-step recovery of metals of interest from nodules using silicothermic reduction with 10% excess silicon over stoichiometry. The phase composition, microstructure and mechanical properties of the obtained reduced material were determined.

Keywords: Deep-sea nodules, Silicothermic reduction, Microstructure

1 Introduction

Deep-sea nodules are polymetallic oxide ores that mainly contain manganese, iron, nickel, copper, and smaller amounts of other elements, such as rare earth metals [1-3]. The composition of the nodules varies depending on the place of occurrence, altogether more than 40 different elements were found in the nodules, the representation changes depending on the place of origin [4]. The following factors have a major influence on metals in polymetallic nodules: the number of metals present in a given area (in the ocean), structure and dynamics of water, relief of the bottom and depth at which the nodules are deposited [5]. The processing of deep-sea nodules is carried out as an extraction of the metals contained in them. Nowadays, two types of extraction procedures are used to obtain the metal of interest – pyrometallurgical process, followed by hydrometallurgical process, or hydrometallurgical treatment (leaching) only [6, 7].

Metallothermy is a process in which reduction occurs, using metals with a high affinity for oxygen as the reducing agent. During metallothermic reduction, metal oxide (MeO) is reduced by a metal reducing agent, which then turns into an oxide. Among the most commonly used reducing agents are aluminium and silicon, but in certain cases magnesium or calcium can be used [8]. Silicothermic reduction, or the reduction of metal oxides by silicon, is less common compared to aluminothermic reduction, where aluminium is used for reduction. One example where silicothermic reduction is applied is in the production of ferroalloys in an electric arc furnace. Silicon as the reducing agent was also used in the production of silicon carbide nanocomposites [9]; the material with high electrical conductivity created in this way was used to produce the negative electrodes of lithium-ion batteries, which had an increased storage capacity. One of the reasons why silicon can be used as suitable reducing agent is its position in the Ellingham diagram which is located at the bottom. It can be read from this diagram that the lower the ΔG of the reaction, the more stable is the oxide. In the lower part of the diagram there are stable oxides, while in the upper part there are less stable oxides that can be easily reduced and decompose to form oxygen even at relatively low temperatures. These oxides located above in the diagram are not very stable and can be easily reduced. In general, a given element can reduce all oxides that are higher in the diagram than the corresponding element's oxide [8].

In this work, microstructure, mechanical properties and phase composition of new alloys produced by silicothermic reaction from deep-sea nodules were tested. Obtained results were compared with articles on the aluminothermic reduction of deep-sea nodules [4, 7].

2 Experimental

The deep-sea nodules were crushed to a powder with particle size under 125 μm. The chemical composition of the nodules was measured by X-ray fluorescence spectrometer (XRF, Axios, PANanalytical, Almelo, The Netherlands) and it is presented in the Tab. 1.

Tab. 1 *Chemical composition (XRF) of the deep-sea nodules (in wt. %)*

Element	Mn	Si	Fe	Al	Na	Ni	Mg	Ca	Cu	Cl	K	Ba	O
[wt. %]	52.41	12.83	10.45	4.45	3.39	2.87	2.70	2.50	2.38	1.44	1.44	1.05	bal.

Using equations based on the Ellingham diagram, the stoichiometric amount of silicon required for silicothermic reduction was calculated [4, 7]. According to the calculation, 32 g of silicon had to be used for 100 g of nodules. In this work, metallothermic reduction was carried out with a 10% excess of silicon over stoichiometry, i.e. 35.2 g of silicon for 100 g of nodules. For metallothermic reduction with 10% excess of silicon over stoichiometry, 295.8 g of nodules and 104.2 g of silicon were prepared in a crucible, for a total of 400 g of nodules with silicon.

The silicothermic reactions were initiated by the mixture composed of silicon powder, nodules, sodium peroxide and magnesium metal flakes. After the reaction was completed, metallic alloy and slag were obtained by mechanical separation. The metal particles were divided into two groups based on the fracture colour: gold and silver samples. Both sample types were further examined using the procedure described below.

The phase composition of material was determined by powder X-ray diffraction (XRD). Data in Bragg–Brentano geometry were collected on a X'Pert3 Powder diffractometer using CuKα radiation. The metallographic cross-sections were ground on SiC abrasive papers P60-P1200. After etching the sample with Kroll's reagent (HF, HNO_3, H_2O), the microstructure was observed using an Eclipse MA200 metallographic optical microscope (Nikon, Tokyo, Japan) and by scanning electron microscope (SEM) VEGA 3 LMU (TESCAN, Brno, Czech Republic). The scanning electron microscope is equipped with energy-dispersive spectrometer (EDS) X-max 20 mm² detector (Oxford Instruments, High Wycombe, UK) was applied.

In addition to the phase analysis and microstructure evaluation, the samples were characterized from the viewpoints of mechanical properties (microhardness). Microhardness was measured by the Vickers method at a load of 100 g (HV 0.1), which corresponds to 0.98 N. This load was used for determination of the hardness of individual phases. Furthermore, a load of 1 000 g (HV 1) was used to determine the hardness of the samples.

3 Results and discussion

3.1 Silicotermic reduction

According to X-ray diffraction analysis (Fig. 1), the metal sample in reduced state contains three phases, which are MnSi, Mn_5Si_3 a Mn. Phase MnSi (cubic, $P2_13$ space group, a = 0.456 × 10^{-10} m) is. Phase Mn_5Si_3 (hexagonal, P63/mcm space group, a = 0.689 × 10^{-10} m, c = 0.479 × 10^{-10} m). According to the Mn-Si diagram, MnSi and Mn_5Si_3 contain 34 and 24 wt.% Si, respectively. The Mn phase is in the diagram in two modifications – α and β. In this case, the sample is a β-Mn modification (primitive cubic, $P4_132$ space group).

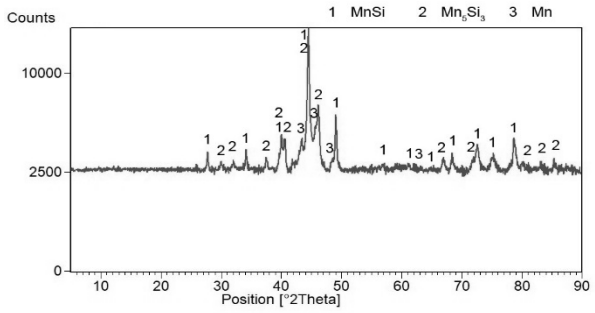

Fig. 1 *X-ray diffraction pattern of a metal sample*

The microstructure of the sample with a gold colour of the fracture surface is shown in Fig. 2. The matrix phase in this case is dark and sharp-edged particles begin to form in it. These white particles are silicides MnSi. The sharp-edged morphology of these particles is due to the tangential growth mechanism.

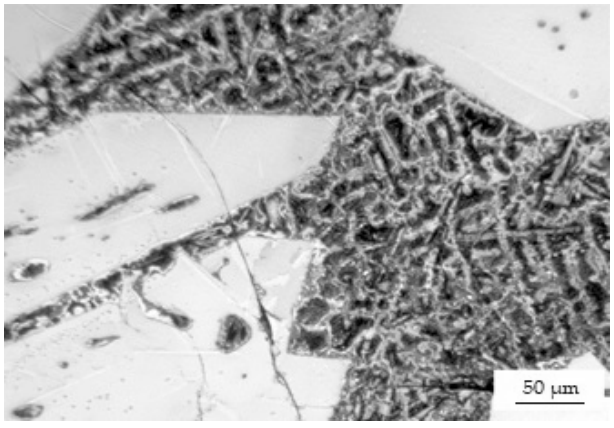

Fig. 2 *The microstructure of the sample with a gold fracture*

In the Fig. 3 the microstructure of the sample with a gold fracture is shown in the scanning electron micrograph. There is possible to see the phase with silicon. The matrix phase is rich in the presents of manganese. According to an EDS, which is shown in the Fig. 4 is the matrix phase also rich in nickel and copper. This means, that this phase is according to the XRD patterns β-Mn, but the chemical composition of that phase is completely different. It can be seen from Fig. 4 that the grain boundaries are rich in phosphorus. Silicon occurs in the matrix phase in lower amount, probably located in Mn_5Si_3 carbide particles dispersed in β-Mn. The hardness of this sample was 1193 ± 40 HV1.

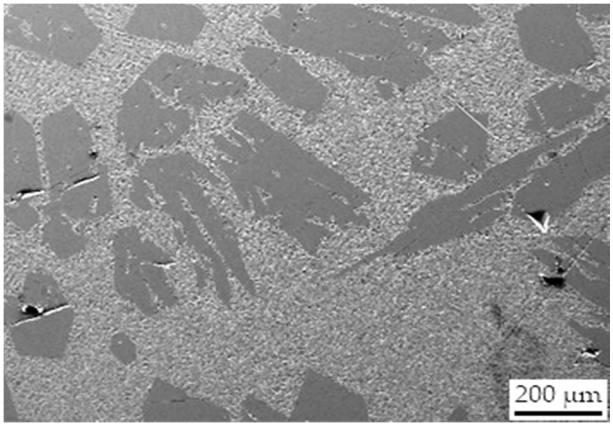

Fig. 3 *The microstructure of the sample with a gold fracture in the electron microscopy*

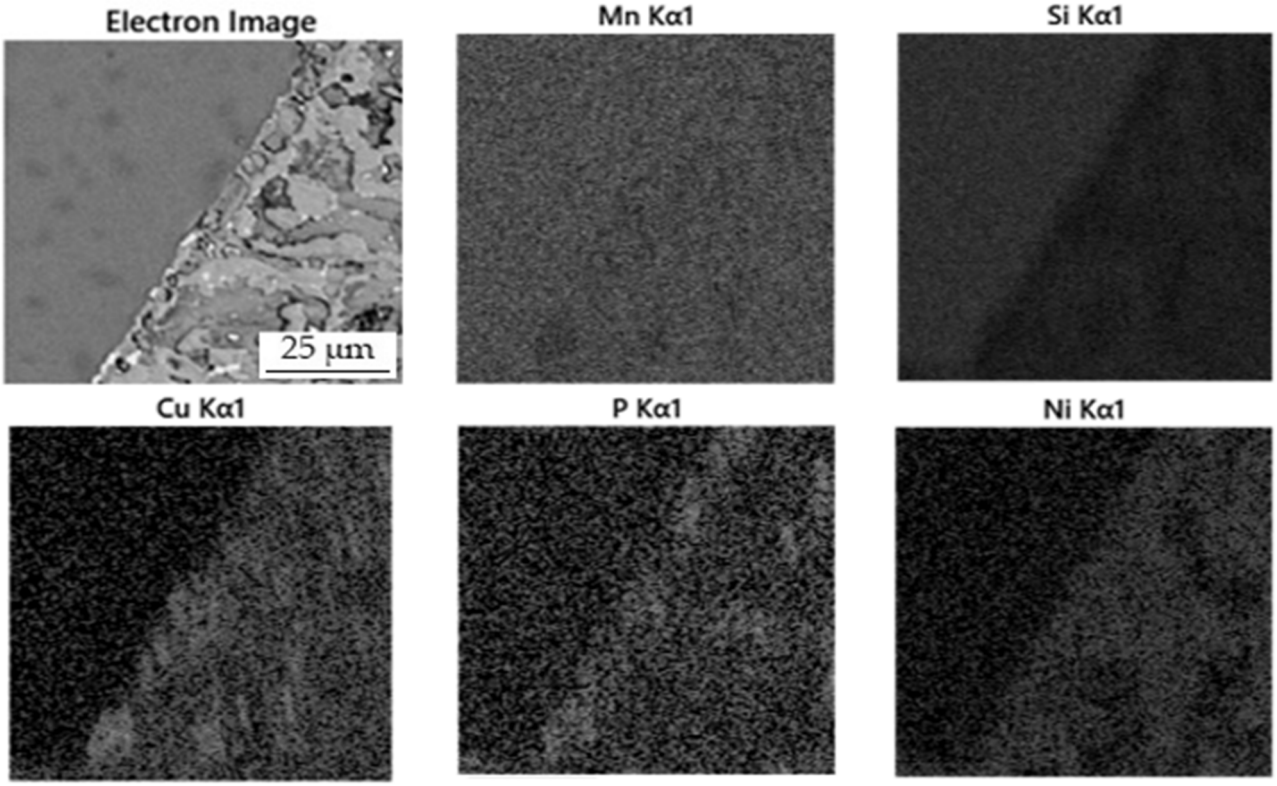

Fig. 4 *EDS map of the distribution of the elements in the microstructure of the sample with a gold fracture*

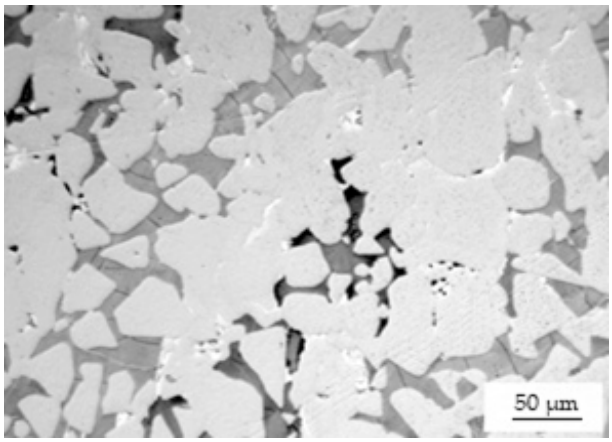

Fig. 5 *The microstructure of the sample with a silver fracture*

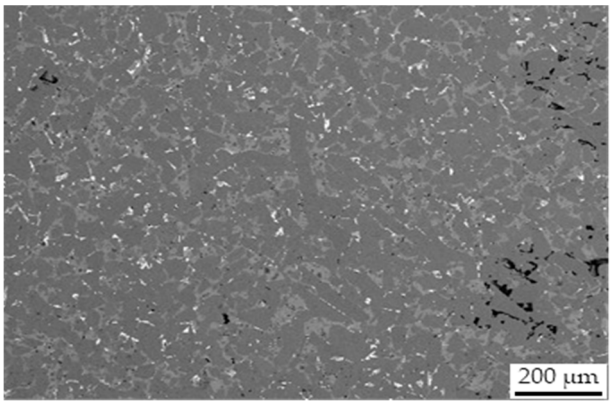

Fig. 6 *The microstructure of the sample with a silver fracture in the electron microscopy*

Fig. 5 shows the microstructure of the silver fracture sample. The resulting phases are not sharp compared to the previous structure. In this sample, the structure is finer-grained and more homogeneous. The matrix phase is dark in Fig. 5, and light phases that are rich in silicon begin to form in it.

In Fig. 6, the microstructure of the silver fracture sample is visible in the backscattered electron microscope. Bright spots can be seen here, which according to the elemental map in Fig. 7 are rich in copper. The matrix is a phase with a higher manganese content. It is therefore a β-Mn phase. The silicide phase with rounded edges is Mn_5Si_3 according to the EDS analysis.

The hardness of the β-Mn phase is 847 ± 40 HV 0.1. The hardness of the silicide phase is 1173 ± 31 HV 0.1. In this case, there is not such a striking difference in hardness between the individual phases of one sample.

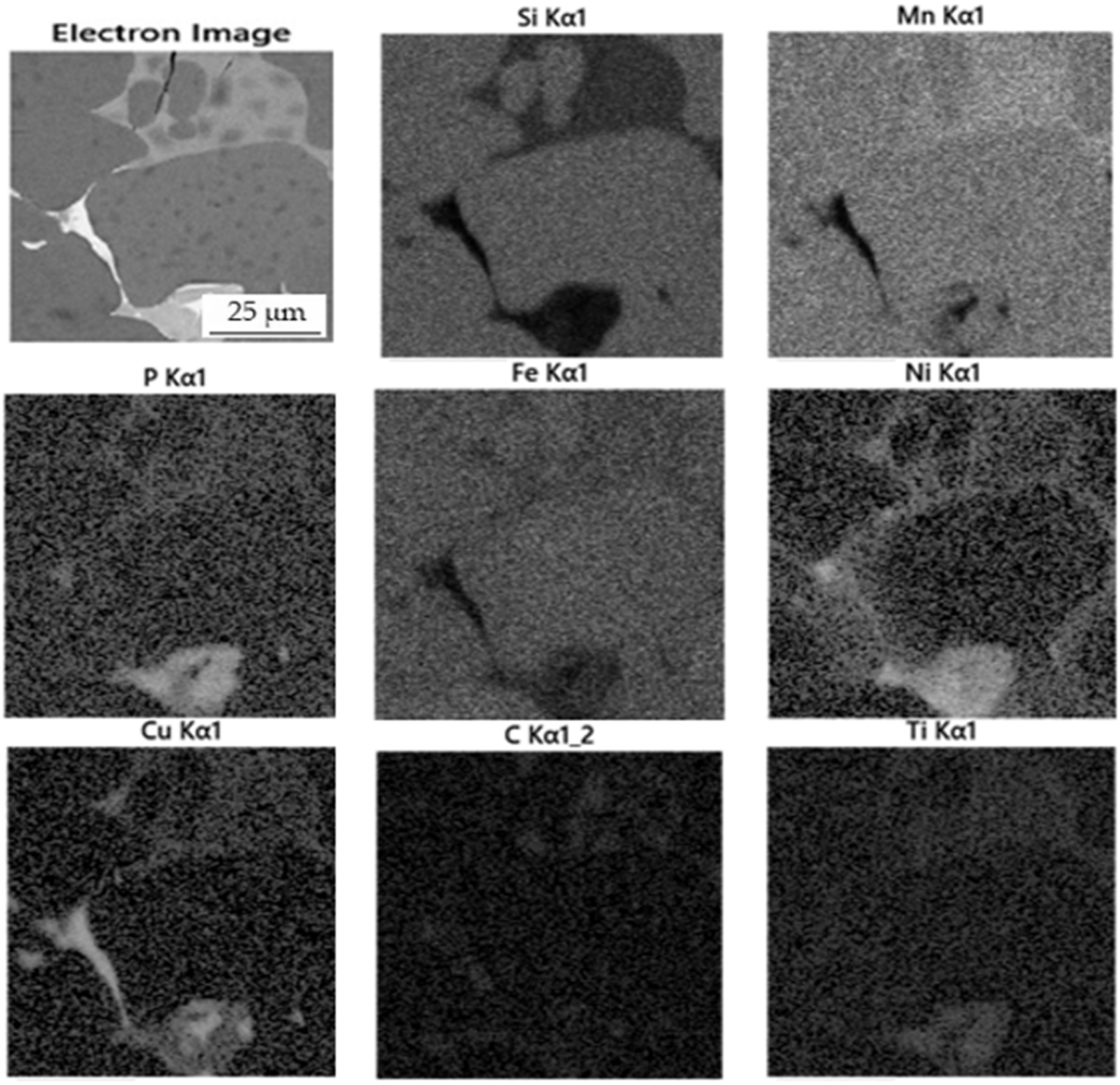

Fig. 7 *EDS map of the distribution of the elements in the microstructure of the sample with a silver fracture*

3.2 Comparison of silicothermic and aluminothermic reduction

Based on the XRD patterns, it can be concluded that the sample that was reduced by silicon contained two types of manganese silicide MnSi and Mn_5Si_3 and the β-Mn phase, while the sample that was reduced by aluminium with 10% excess of aluminium over stoichiometry [4] contained β-Mn as a major phase, two phases with crystal structure of Heusler phases Mn_2FeSi (22 wt. %) and Mn_2FeAl (17 wt. %). In this sample, there were also two minor phases $Mn_{0.83}Si_{0.11}$ (R-3) and Mn_2P (P-62m) with only 6 wt. % combined.

From the measured results, it can be said that during silicothermic reduction and aluminothermic reduction, a 10% excess of the given element is the result of the β-Mn matrix phase. However, the hardness of these phases is significantly different for aluminothermic and silicothermic reduction [4]. For aluminium-reduced samples, the microhardness was around 750 HV 0.1, while for silicon-reduced samples, the hardness was around 1000 HV 0.1. In general, it can be stated that the sample created by silicothermic reduction has a higher hardness compared to the sample created by aluminothermic process. The reason is probably the high content of hard silicides in the silicothermically reduced sample.

4 Conclusions

The silicothermic reduction of deep-sea nodules lead to the formation of two different metallic phases, differing in the appearance of the fracture surface. Based on the XRD analysis of the whole metallic product, it can be concluded that the sample that was reduced by silicon contained two types of manganese silicide MnSi and Mn_5Si_3 and the β-Mn phase. It can be stated that the sample with gold fracture has completely different microstructure than the sample with silver fracture. The sample with the gold fracture surface has the sharp-edged MnSi silicides in the matrix containing mostly β-Mn, probably with dispersed Mn_5Si_3 particles. On the other hand, almost rounded Mn_5Si_3 blocky silicide particles in the β-Mn based matrix arose in the metallic product with the silver fracture.

Acknowledgement

This research was funded by Czech Science Foundation, project No. 20-15217S.

References

[1] VERESHCHAGIN, O.S.; PEROVA, E.N.; BRUSNITSYN, A.I.; ERSHOVA, V.B.; KHUDOLEY, A.K.; SHILOVSKIKH, V.V.; MOLCHANOVA, E.V. (2019). Ferro-manganese nodules from the Kara Sea: Mineralogy, geochemistry and genesis. In: *Ore Geology Reviews*, 106, 192-204

[2] MSALLAMOVÁ, Š.; NOVÁK, P.; MIOSSEC, P.; KOPEČEK, J.; TSEPELEVA, A.; RUDOMILOVA, D.; FOJT, J. (2021). Corrosion Properties of Mn-Based Alloys Obtained by Aluminothermic Reduction of Deep-Sea Nodules. In: *Materials*, 14

[3] NOVÁK, P.; VLÁŠEK, J.; DVOŘÁK, P.; ŠKOLÁKOVÁ, A.; NOVÁ, K.; KNAISLOVÁ, A. (2020) Microstructure of the alloys prepared by reduction of deep-sea nodules by aluminium and silicon. In: *Manufacturing Technology*, 20, 655–659

[4] NOVÁK, P.; VU, N.H.; ŠULCOVÁ, L.; KOPEČEK, J.; LAUFEK, F.; TSEPELEVA, A.; DVOŘÁK, P.; MICHALCOVÁ, A. (2021) Structure and Properties of Alloys Obtained by Aluminothermic Reduction of Deep-Sea Nodules. In: *Materials*, 14

[5] MICHALCOVÁ A.; ORLÍČEK M.; NOVÁK P. (2021) Aluminum Alloys with the Addition of Reduced Deep-Sea Nodules. In: *Metals*, 2021. 11(3)

[6] KNAISLOVÁ, A.; VU, H.; DVOŘÁK, P. (2018) Microwave and Ultrasound Effect on Ammoniacal Leaching of Deep-Sea Nodules. In: *Minerals*, 8

[7] BORKOVCOVÁ, K.; NOVÁK, P. (2022) Possibilities of a Direct Synthesis of Aluminum Alloys with Elements from Deep-Sea Nodules. In: *Materials*, 15

[8] JANDOVÁ, J.; VU, N.H.; DVOŘÁK, P. (2018) *Metody Výroby Neželezných Kovů a Zpracování Odpadů*; Vysoká Škola Chemicko-Technologická v Praze: Prague, Czech Republic

[9] ASTROVA, E.V.; ULIN, V.P.; PARFENEVA, A.V.; RUMYANTSEV, A.M.; VORONKOV, V.B.; NASHCHEKIN, A.V.; NEVEDOMSKIY, V.N.; KOSHTYAL, Y.M.; TOMKOVICH, M.V. (2020) Silicon–carbon nanocomposites produced by reduction of carbon monofluoride by silicon. In: *Journal of Alloys and Compounds*, 826